

Fed-Batch Microbioreactor Platform for Scale Down and Analysis of a Plasmid DNA Production Process

Diana M. Bower,¹ Kevin S. Lee,² Rajeev J. Ram,² Kristala L.J. Prather¹

¹Department of Chemical Engineering, Massachusetts Institute of Technology, 77 Massachusetts Ave., Room 66-454, Cambridge, Massachusetts 02139; telephone: 617-253-1950; fax: 617-258-5042; e-mail: kljp@mit.edu

²Research Laboratory of Electronics, Massachusetts Institute of Technology, Cambridge, Massachusetts

ABSTRACT: The rising costs of bioprocess research and development emphasize the need for high-throughput, low-cost alternatives to bench-scale bioreactors for process development. In particular, there is a need for platforms that can go beyond simple batch growth of the organism of interest to include more advanced monitoring, control, and operation schemes such as fed-batch or continuous. We have developed a 1-mL microbioreactor capable of monitoring and control of dissolved oxygen, pH, and temperature. Optical density can also be measured online for continuous monitoring of cell growth. To test our microbioreactor platform, we used production of a plasmid DNA vaccine vector (pVAX1-GFP) in *Escherichia coli* via a fed-batch temperature-inducible process as a model system. We demonstrated that our platform can accurately predict growth, glycerol and acetate concentrations, as well as plasmid copy number and quality obtained in a bench-scale bioreactor. The predictive abilities of the micro-scale system were robust over a range of feed rates as long as key process parameters, such as dissolved oxygen, were kept constant across scales. We have highlighted plasmid DNA production as a potential application for our microbioreactor, but the device has broad utility for microbial process development in other industries as well.

Biotechnol. Bioeng. 2012;109: 1976–1986.

© 2012 Wiley Periodicals, Inc.

KEYWORDS: microbioreactors; *Escherichia coli*; plasmid biopharmaceuticals; bioprocess development

Introduction

There is increasing pressure in the pharmaceutical industry to accelerate the discovery-to-launch timelines for therapeutics and to reduce the cost of research and development. It can be difficult to realize cost savings when dealing with biological therapeutics, as their development often entails extensive process design and scale-up studies using bench-top bioreactors. Other cheaper, more high-throughput process development tools exist (shake flasks and micro-well plates), but they often sacrifice process monitoring and control capabilities for cost and throughput savings.

With these challenges in mind, many researchers have sought to design mini- and microbioreactors that maintain the control and monitoring capabilities of bench-scale units while increasing throughput and decreasing capital and labor costs. These developments typically occur in one of several forms: miniaturized stirred-tank reactors with working volumes on the order of milliliters, micro-well plates that have been modified to allow online process monitoring and/or nutrient feeding, or flat-form micro-fluidic devices with microliter-scale working volumes. The state-of-the-art in microbioreactor development has been reviewed recently, with articles focusing on the breadth of available reactor configurations (Betts and Baganz, 2006), as well as advances in process monitoring and fabrication techniques (Schapper et al., 2009). Another recent article reviewed all of the available small-scale process development tools and outlined the features that an ideal scale-down system should contain to meet current biopharmaceutical process development needs (Bareither and Pollard, 2011).

Since the first report of a micro-scale fermentation device over a decade ago (Kostov et al., 2001), tremendous progress has been made in the design of microbioreactors. However, only recently have more complex process strategies, such as fed-batch operation, been investigated at the microscale. Fed-batch processes are common in industrial fermentation

Correspondence to: K.L.J. Prather

Contract grant sponsor: MIT-Portugal Program

Contract grant sponsor: Pfizer, Inc.

Contract grant sponsor: National Science Foundation

Received: 23 January 2012; Revision received: 7 March 2012;

Accepted 8 March 2012

Accepted manuscript online 15 March 2012;

Article first published online 30 March 2012 in Wiley Online Library

(<http://onlinelibrary.wiley.com/doi/10.1002/bit.24498/abstract>)

DOI 10.1002/bit.24498

and cell culture as they facilitate a significant increase in biomass under controlled-growth-rate conditions, often leading to increased productivity. Reports of fed-batch processes at the microscale vary in their complexity. Isett et al. (2007) achieved feeding in the 24-well μ -24 system (Applikon Biotechnology Inc., Foster City, CA) by manually removing the reactor cassette and adding substrate aseptically in a biosafety cabinet. Other devices at both the microliter and milliliter scale have used robotics to intermittently add feed solution to the microreactor cultures (Legmann et al., 2009; Vester et al., 2009). Siurkus et al. (2010) sought to achieve more continuous feeding using the Enbase controlled-release technology (Panula-Perala et al., 2008) to mimic a fed-batch process in 96-well plates used for high-throughput library screening. Implementing a fed-batch process early on allowed the group to not only select a high-producing cell line, but to ensure that the associated conditions would maintain productivity upon scale-up. Microfluidics have also been used for nutrient feeding as demonstrated by Funke et al. (2010). These researchers coupled microfluidic channels to the microtiter plates in the BioLector system (m2p-labs GmbH, Baesweiler, Germany) to achieve a fed-batch process.

In this work, we have adapted a microbioreactor system originally designed for continuous culture (Lee et al., 2011) for fed-batch cultivation of *Escherichia coli* bearing a plasmid DNA vaccine vector. Plasmid-based DNA vaccines have been gaining attention as promising therapies for many human diseases (Kutzler and Weiner, 2008), and as a result there has been significant work on the design of high-yield, high-quality production processes for this class of biopharmaceuticals. We chose to study a plasmid production process in the microbioreactors because of its complexity—plasmid amplification is induced by a temperature shift, and plasmid DNA is an intracellular product that can only be measured offline. Our microbioreactor is capable of real-time monitoring and control of pH, dissolved oxygen, and temperature, as well as online measurement of optical density. Substrate feeding can also be accurately controlled by the system. A working volume of 1,000 μ L allows periodic sampling for offline analysis of metabolites and the plasmid DNA product. This work characterizes the features of our fed-batch microbioreactor and demonstrates its utility as a process design tool in the context of plasmid DNA production.

Materials and Methods

Plasmid and Strain

This study used *E. coli* DH5 α [F^- ϕ 80*lacZ* Δ M15 Δ (*lacZYA-argF*)U169 *deoR recA1 endA1 hsdR17*(r_k^- , m_k^+) *phoA supE44 thi-1 gyrA96 relA1* λ^-] as a host for the plasmid pVAX1-GFP. pVAX1-GFP is a 3,642-bp, kanamycin-resistant plasmid constructed by cloning the superfolder green fluorescent protein gene (Pedelacq et al., 2006) into the

multi-cloning site of pVAX1 (Invitrogen, Carlsbad, CA), a pUC-based DNA vaccine vector backbone. DH5 α [pVAX1-GFP] frozen seed banks were prepared from mid-exponential-phase shake flask cultures grown at 30°C and stored at -80°C in 15% glycerol.

Culture Medium

A semi-defined culture medium was adapted from Listner et al. (2006). The basal cultivation medium contained 3 g/L (NH₄)₂SO₄, 3.5 g/L K₂HPO₄, 3.5 g/L KH₂PO₄, 10 g/L yeast extract, and 10 g/L Bacto peptone. 5 g/L glycerol, 8.3 mL/L seed supplement solution, 1 mL/L trace elements solution, and 25 μ g/mL kanamycin were added as supplements to the basal medium. The seed supplement solution contained 60 g/L MgSO₄·7H₂O and 24 g/L thiamine hydrochloride. The trace elements solution contained 16.2 g/L FeCl₃, 2 g/L ZnCl₂, 2 g/L CoCl₂·6H₂O, 2 g/L Na₂MoO₄·2H₂O, 1 g/L CaCl₂·2H₂O, 1.27 g/L CuCl₂·2H₂O, and 0.5 g/L H₃BO₃ dissolved in 1.2 N hydrochloric acid. The pH of the basal medium was adjusted to 7.1 using NaOH. The feed solution for all fed-batch cultures contained 321.4 g/L glycerol and 79.3 g/L yeast extract.

Plasmid DNA Production Process

pVAX1-GFP was produced in a process adapted from Carnes et al. (2006) that consisted of three phases: (1) batch growth on 5 g/L glycerol at 30°C, (2) feeding of a concentrated glycerol/yeast extract solution at 30°C, and (3) plasmid amplification at 42°C with continued feeding.

Microbioreactor Device Design

The fed-batch microbioreactor device used in this study (Fig. 1) was a modified version of the continuous culture device designed by Lee et al. (2011). In contrast to the continuous device, the fed-batch microreactor has three 15- μ L fluid reservoirs connected to the growth chamber via peristaltic pumps, each with an injection volume of 240 nL. The pumps share the three valves required for operation (Lee et al., 2011), while the input to the pumps is selected by independent upstream valves (Fig. 1B: V2–V4). In another key adaptation from the continuous culture device, each reservoir was given a direct connection to the growth chamber by removing the pass-through channel and combiner before the peristaltic pump. This reduced the time delay between performing an injection and the injected plug of liquid reaching the growth chamber. As in the continuous device, the growth chamber consists of three interconnected sections, each with a 500- μ L liquid capacity. Using a working volume of 1,000 μ L ensured that at most only two of the sections were full at a given time to facilitate mixing. Oxygenation of the growth chamber was provided by gas diffusion through the PDMS membrane and was

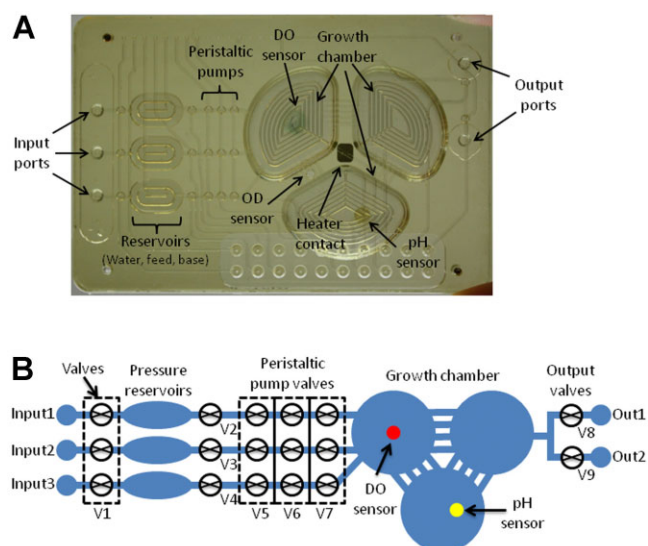


Figure 1. A: Photograph of the fed-batch microbioreactor device with key features indicated. B: Schematic of the microbioreactor highlighting details of the liquid flow path and valve design. The dotted boxes indicate that the valves are shared and act as a single unit. Valves are numbered V1–V9. V1 controls flow from the solution input bottles (water, feed, and base); V2–V4 allow selection of output from pressurized reservoirs; V5–V7 comprise the peristaltic pumps; V8 and V9 control output from device. The reservoirs also have a shared valve for pressurization (not shown).

enhanced by mixing (Lee et al., 2006b). Samples for offline analysis were collected via one of two output ports connected to the growth chamber (Fig. 1).

Heating was performed at the base of the device using a resistive heater and a digital temperature sensor calibrated against the temperature of water inside the reactor. Dissolved oxygen and pH sensing were performed as described by Lee et al. (2011). Optical density was measured through a 100- μm path length at a wavelength of 590 nm by positioning an LED and photodetector in-line in a connecting microchannel between two of the growth chamber sections. A smaller path length enabled linear optical density measurements up to at least $\text{OD}_{600} = 50$ as measured offline by a DU800 Spectrophotometer (Beckman Coulter, Indianapolis, IN). All optical sensors were measured using fiber optic probes and data was analyzed in MATLAB to extract measured values. Oxygen and temperature control algorithms were implemented using PID control (Lee et al., 2011) while pH control was implemented using a threshold and estimation algorithm (Lee et al., 2004).

Microbioreactor Cultures

Prior to use, the microbioreactors were placed in heat-sealable PVC bags and sterilized by gamma-irradiation at 18 kGy. To prepare inoculum for the microbioreactors, 3 mL of semi-defined medium was inoculated with 0.4% seed

bank and grown overnight at 30°C. The next day, 3 mL semi-defined medium was inoculated to an initial OD_{600} of 0.3 using the overnight culture; 1,000 μL of the resultant culture was used to fill the microbioreactor. Dissolved oxygen was controlled by varying the ratio of oxygen and helium in the inlet gas. Helium was used as the inert gas instead of nitrogen because its low solubility in water helped to control foaming. pH was controlled at 7.1 using 4M NaOH. To better mimic the conditions in the bench-scale reactor, the temperature was slowly increased from 30 to 42°C over a period of 30 min during the temperature induction phase of the plasmid production process. An evaporation control scheme was used to compensate for volume lost to evaporation and sampling. Before the start of feeding, the chip entered evaporation refill mode (Lee et al., 2011) every 30 min. After a sample was taken, the reactor was manually set to evaporation refill mode to add sterile distilled, de-ionized water until the culture reservoir was full. Evaporation refill was turned off after the start of feeding (approximately 8 h after inoculation) to help maintain the reactor volume at or below 1 mL. Working volumes above 1 mL could result in reduced mixing efficiency. During the 30°C feeding phase, the feed addition helped compensate for volume lost due to evaporation; however, evaporation control was turned back on after the temperature shift (at approximately 20 h) to compensate for the higher evaporation rate at the elevated temperature. While this scheme may have resulted in some transient changes in nutrient concentration, it helped alleviate the large volume losses observed in runs without any compensation for evaporation. At the end of the process, the chip could be discarded or gamma-irradiated and re-used.

Bioreactor Cultures

Bench-scale bioreactor cultures were performed using a Labfors 3 bioreactor (Infors, Bottmingen, Switzerland) with a maximum working volume of 2.3 L. The bioreactor was equipped with a D140 OxyProbe dissolved oxygen sensor (Broadley-James, Irvine, CA) and an F-695 FermProbe pH electrode (Broadley-James). To prepare the bioreactor inoculum, 3 mL of semi-defined medium was inoculated with 0.4% seed bank and grown overnight at 30°C. The next day, 100 mL of semi-defined medium was inoculated with 100 μL of overnight culture in a 500-mL baffled shake flask and incubated overnight at 30°C.

To set up the bioreactor, 1.3–1.8 L of basal cultivation medium was autoclaved in the reactor. On the day of inoculation, medium supplements and 0.2 mL Antifoam 204 (Sigma–Aldrich, St. Louis, MO) were added, and the reactor was inoculated to an initial OD_{600} of 0.3 using overnight seed culture. The dissolved oxygen setpoint was controlled at 35% using a cascade to agitation (250–800 rpm), and air was provided at an initial flow rate of 1 vvm. For oxygen supplementation studies, pure oxygen was automatically added to the air flow at 0.4–0.6 LPM as needed to maintain

the DO setpoint. In all runs, the air flow was increased to 1.2 vvm when the temperature was increased to 42°C. pH was controlled at 7.10 ± 0.05 using 4 M NaOH and 2.25 M H₃PO₄. Online data was logged using IRIS fermenter log and control software (Infors). Antifoam was manually added in 0.2-mL increments as needed. Samples were taken periodically to measure OD₆₀₀ offline using a DU800 Spectrophotometer (Beckman Coulter). Samples for glycerol, acetate, and plasmid DNA concentration measurements were stored at -30°C until analysis.

Measurement of Glycerol and Acetate Concentrations

Glycerol and acetate concentrations in culture supernatants were determined using an Agilent 1200 Series HPLC (Agilent Technologies, Santa Clara, CA) equipped with an Aminex HPX-87H column (Bio-Rad, Hercules, CA). A 5 mM sulfuric acid mobile phase was run at 0.6 mL/min for 25 min at 50°C. Glycerol and acetate peaks were detected by refractive index at approximate retention times of 13.4 and 15.2 min, respectively.

Measurement of Plasmid Copy Number

Plasmid copy number was measured using a quantitative PCR (qPCR) assay adapted from the relative quantitation method described by Lee et al. (2006a). Total DNA (genomic and plasmid) was isolated from 25 to 50 µL of culture using the DNeasy Blood & Tissue kit (Qiagen, Valencia, CA). qPCR was performed using a 7300 Real-Time PCR system (Applied Biosystems, Carlsbad, CA) with primers targeting the plasmid-based kanamycin resistance gene (forward primer: 5'-TCGACCACCAAGCGAAACA-3', reverse primer: 5'-CGACAAGACCGGCTTCCAT-3') and *dxs*, a single-copy gene on the *E. coli* chromosome encoding 1-deoxyxylulose-5-phosphate synthase (forward primer: 5'-CGAGAAACTGGCGATCCTTA-3', reverse primer: 5'-CTTCATCAAGCGTTTCACA-3'). Each 25-µL qPCR reaction contained 1X Brilliant II SYBR Green High ROX Master Mix reagent (Agilent Technologies), 200 nM each of the forward and reverse primers, and the total DNA sample diluted 10- to 100-fold in order to be within the linear range of the assay. The thermal profile consisted of a 10-min hold at 95°C followed by 40 cycles of 95°C for 30 s and 60°C for one minute. Plasmid copy number was calculated using the $\Delta\Delta C_T$ method (Livak and Schmittgen, 2001), which included normalization to a calibrator plasmid, pVAX1-*dxs*, containing single copies of both the kanamycin resistance gene and *dxs*.

Measurement of Plasmid DNA Specific Yield

Plasmid DNA was quantified from crude lysates prepared from OD₆₀₀ = 10 cell pellets using the method described by Listner et al. (2006). Typically, volumes ranging from 0.2 to 2.5 mL were required to form a pellet of the appropriate

density. The lysis method was modified slightly: cell pellets were harvested by centrifugation at 5,000 × g for 15 min, the 37°C incubation took place with 250 rpm shaking, and 5 µL of 10 mg/mL RNase A solution was used per mL of lysate. The pDNA content of the lysates was measured using a Gen-Pak FAX anion-exchange column (Waters Corporation, Milford, MA) on an Agilent 1100 Series HPLC system (Agilent Technologies). Three buffers were used: Buffer A (25 mM Tris-HCl, 1 mM EDTA, pH 8.0), Buffer B (25 mM Tris-HCl, 1 mM EDTA, 1 M NaCl, pH 8.0), and Buffer C (0.04 M H₃PO₄). The LC method was run at a constant flow rate of 0.75 mL/min and consisted of the following steps: (1) linear ramp from 70%:30% A:B to 34%:66% A:B over 10 min, (2) 100% B for 5 min, (3) 100% C for 4.5 min, and (4) 70%:30% A:B for 10 min. Plasmid DNA eluted at a retention time of approximately 11.5 min as detected by absorbance at 260 nm. A standard curve of pVAX1-GFP (2–50 µg/mL) was prepared using pDNA purified using the Hi-Speed QIAfilter Plasmid Maxi Kit (Qiagen) and quantified using a NanoPhotometer (Implen, Westlake Village, CA). A standard curve was used to calculate the µg of pDNA per mL of lysate prepared from each pellet. Specific yield was calculated using the correlation that 1 OD₆₀₀ unit = 0.4 g DCW/L culture.

pDNA Quality Analysis

Plasmid DNA purified using the Zyppy Plasmid Miniprep Kit (Zymo Research Corporation, Irvine, CA) was run on a 0.7% agarose gel and stained with ethidium bromide to visualize the relative quantities of linear, nicked, and supercoiled species. Linear and nicked pDNA standards were made by digesting pVAX1-GFP with the restriction enzyme XhoI or the nicking endonuclease Nt.BstNB1, respectively.

Results and Discussion

Plasmid Production in Bench-Scale Bioreactors as a Model System

A key property of microbioreactors is the ability to predict the behavior of larger scale fermentations. To evaluate the performance of our fed-batch microbioreactor we used production of a pUC-based DNA vaccine vector via temperature-induction as a model system. Specifically, we compared *E. coli* growth, glycerol consumption, acetate production, and plasmid copy number across scales.

At the bench-scale, initial specific feed rates of 2.6, 3.2, 3.5, and 6.1 g glycerol/L/h were investigated. Growth curves show that fed-batch cultures of DH5α[pVAX1-GFP] typically reached OD₆₀₀ values between 40 and 60 under the conditions tested (Fig. 2A). As the feed rate increased, the final OD₆₀₀ decreased, likely due to the increased duration of oxygen limitation at higher feed rates. With air as the only oxygen source, the dissolved oxygen setpoint

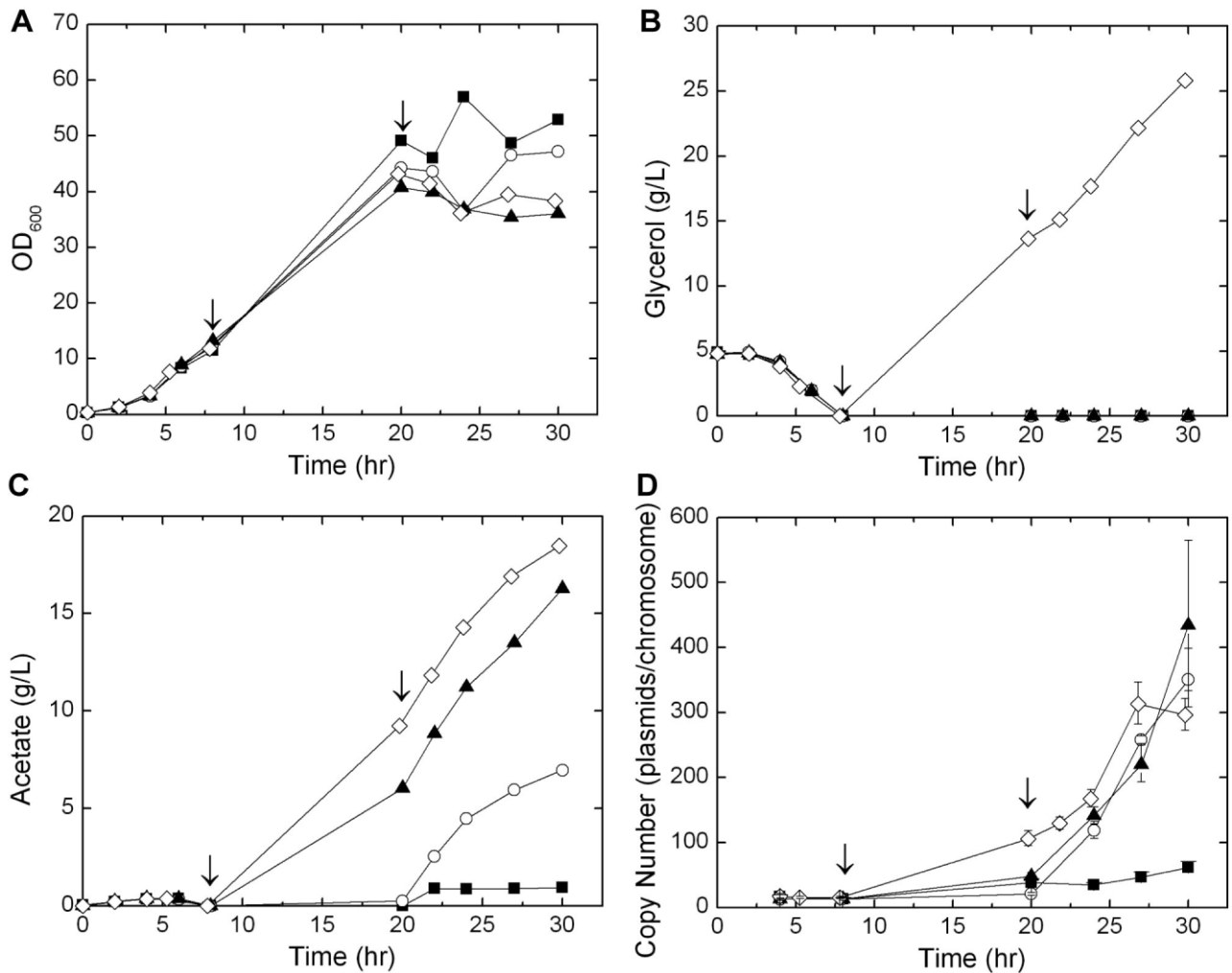


Figure 2. (A) Optical density, (B) glycerol, (C) acetate, and (D) average plasmid copy number profiles for bench-scale fed-batch cultures with initial specific feed rates of 2.6 g glycerol/L/h (■), 3.2 g glycerol/L/h (○), 3.5 g glycerol/L/h (▲), and 6.1 g glycerol/L/h (◇). In each plot, from left to right, the arrows indicate the start of feeding and the 30 to 42°C temperature shift, respectively. The plasmid copy number error bars represent the 95% confidence interval calculated from three replicate wells of the same sample.

could not be maintained for the duration of the run. Higher feed rates led to increased oxygen demand due to increased substrate availability, and as a result, cultures with higher feed rates became oxygen-limited earlier in the run.

In all bench-scale experiments, the 5 g/L of batched glycerol was consumed before the start of feeding (Fig. 2B). At all but the highest feed rate tested, there was no glycerol accumulation in the medium after the start of feeding. Acetate was produced to varying degrees during the feeding phase, with the amount of acetate produced increasing with increasing feed rate (Fig. 2C).

Production of pVAX1-GFP was quantified by measuring the number of plasmid copies per chromosome (Fig. 2D). As expected, temperature-induced amplification of pVAX1-GFP occurred in the bench-scale bioreactor. For the moderate feed rates (3.2 and 3.5 g glycerol/L/h), the plasmid copy number remained below 50 copies/chromosome until

the temperature shift from 30 to 42°C, after which the copy number steadily increased until the end of the fermentation, reaching maximum values of 351 and 434 copies/chromosome, respectively. At the highest feed rate, the copy number was about twofold higher when the temperature was shifted, but clear temperature-induced amplification still occurred. At the lowest feed rate, the plasmid copy number only increased from 39 to 62 copies/chromosome over the course of the temperature-induction phase of the culture. Possible explanations for this phenomenon will be discussed below.

At the bench scale, we were also able to measure specific pDNA yield from crude lysates. The final specific yields were 2.9, 4.5, 1.3, and 0.4 mg pDNA/g DCW at initial specific feed rates of 2.6, 3.2, 3.5, and 6.1 g glycerol/L/h, respectively. There are several possible explanations for the apparent discrepancies between the copy number and specific yield trends. First, conversion between copy number and specific

yield involves several assumptions, including the cellular chromosomal content and the number of intact cells contributing to optical density measurements. The average *E. coli* cell is typically cited to contain 2.1 chromosomes, however, this value was measured for *E. coli* B/r during balanced growth at 37°C, and is not likely to be valid under other growth conditions or for different strains (Neidhardt and Umberger, 1996). Chromosomal content changes with growth rate (Bipatnath et al., 1998) and growth phase (Akerlund et al., 1995) and a twofold change in the number of chromosomes/cell will result in a twofold change in the expected specific yield calculated from a given copy number. Due to the complex nature of cell physiology during non-balanced growth, we cannot calculate the number of chromosomes per cell expected during our fed-batch process. It is also possible that at higher feed rates, cell debris or partially intact cells containing no pDNA contributed to optical density measurements, resulting in an artificial lowering of the specific yield. This is supported by the fact that discrepancies were more prevalent under high-stress culture conditions (oxygen limitation and high acetate concentration) under which cell morphology likely undergoes the most dramatic change. Along these lines, it is also possible that stress-induced physiological and morphological changes reduced the effectiveness of the lysis protocol. Conversely, it is also possible that these physiological changes resulted in partial occlusion of the genomic DNA such that the qPCR primers could not efficiently bind, resulting in reduced detection of the chromosomal target. However, gel electrophoresis analysis of samples from the highest feed rate run showed evidence of increased pDNA concentration with time (data not shown), lending credence to the idea that the specific yield measurements may not be accurately capturing pDNA concentrations.

The apparent discrepancy between the trends in copy number and specific yield observed at the higher feed rates highlights one of the key challenges of microreactor technologies—analytics. The small sample volumes available from the microreactors preclude the use of the specific yield assay. However, the qPCR-based copy number assay can be performed at both scales so we chose to make this our standard for comparison of productivity in the sections that follow.

Plasmid Production in Microbioreactors

Microbioreactor feed rates of 0.536, 0.664, and 0.868 injections per minute were investigated to determine the ability of the microreactors to predict trends in growth, metabolite concentration, and product yield at the bench scale. The volume of each feed injection was approximately 240 nL, but this number varied by roughly 20% due to small deviations in the device fabrication process. The injection rates studied corresponded to specific feed rates of approximately 2.5, 3.1, and 4.0 g glycerol/L/h.

The growth curves at each feed rate (Fig. 3A) demonstrate that the microbioreactors can support cell densities of at least $OD_{600} = 40\text{--}60$. These cell densities are in the range of those observed at the bench scale. Note that the trend in optical density with respect to feed rate is inverted for the microreactors when compared to the bench-scale bioreactor. This is likely due to differences in oxygen availability. The inlet gas stream to the microreactors was supplemented with oxygen, allowing the dissolved oxygen level to be maintained at approximately 30% for all feed rates investigated. Therefore, at higher feed rates, more substrate was available for biomass production and its utilization was not restricted by the oxygen limitation observed at the bench scale.

The glycerol profiles from the microreactor experiments (Fig. 3B) show that, in contrast to the bench-scale runs, there was some glycerol present at the time feeding began. The highest feed rate resulted in glycerol accumulation, suggesting that the cells were unable to utilize all of the glycerol being fed. However, the glycerol concentration decreased after the temperature shift, suggesting an increase in glycerol uptake rate. This is in contrast to the bench-scale reactor in which glycerol accumulated in the medium monotonically.

The acetate accumulation profiles (Fig. 3C) highlight a major difference observed between the micro and bench scales. With the exception of the highest feed rate tested, less than 1 g/L acetate was produced in the microreactors. This is in stark contrast to the bench-scale reactor in which acetate accumulated under all conditions tested (Fig. 2C).

Temperature-induced amplification of pVAX1-GFP was observed at feed rates of 0.536 and 0.664 injections/min in the microreactors (Fig. 3D). The final copy number values were about twofold lower than those observed at the bench scale; however, a comparison by agarose gel electrophoresis shows comparable pDNA content across the reactor scales (Fig. 4: Lanes 4, 5, and 7). At a feed rate of 0.868 injections/min there was a slight increase in copy number after the temperature shift, but the increase was not nearly as dramatic as that observed at the lower feed rates or at the bench scale.

Additional experiments demonstrated that the residual glycerol present at the time of feed initiation in the microreactor did not impact plasmid copy number (data not shown). Delaying feeding resulted in a slight increase in the maximum acetate concentration (1.3 g/L compared to 0.5 g/L, both at 20 h), but the final acetate concentrations with both feeding schemes were nearly identical.

Another factor that could be contributing to the differences observed between scales is that in the microreactors the volume was kept approximately constant at 1,000 μL throughout the run, and as a result the specific feed rate remained the same. This is in contrast to the bench-scale reactor in which the specific feed rate decreased over the course of the fermentation due to the increasing culture volume.

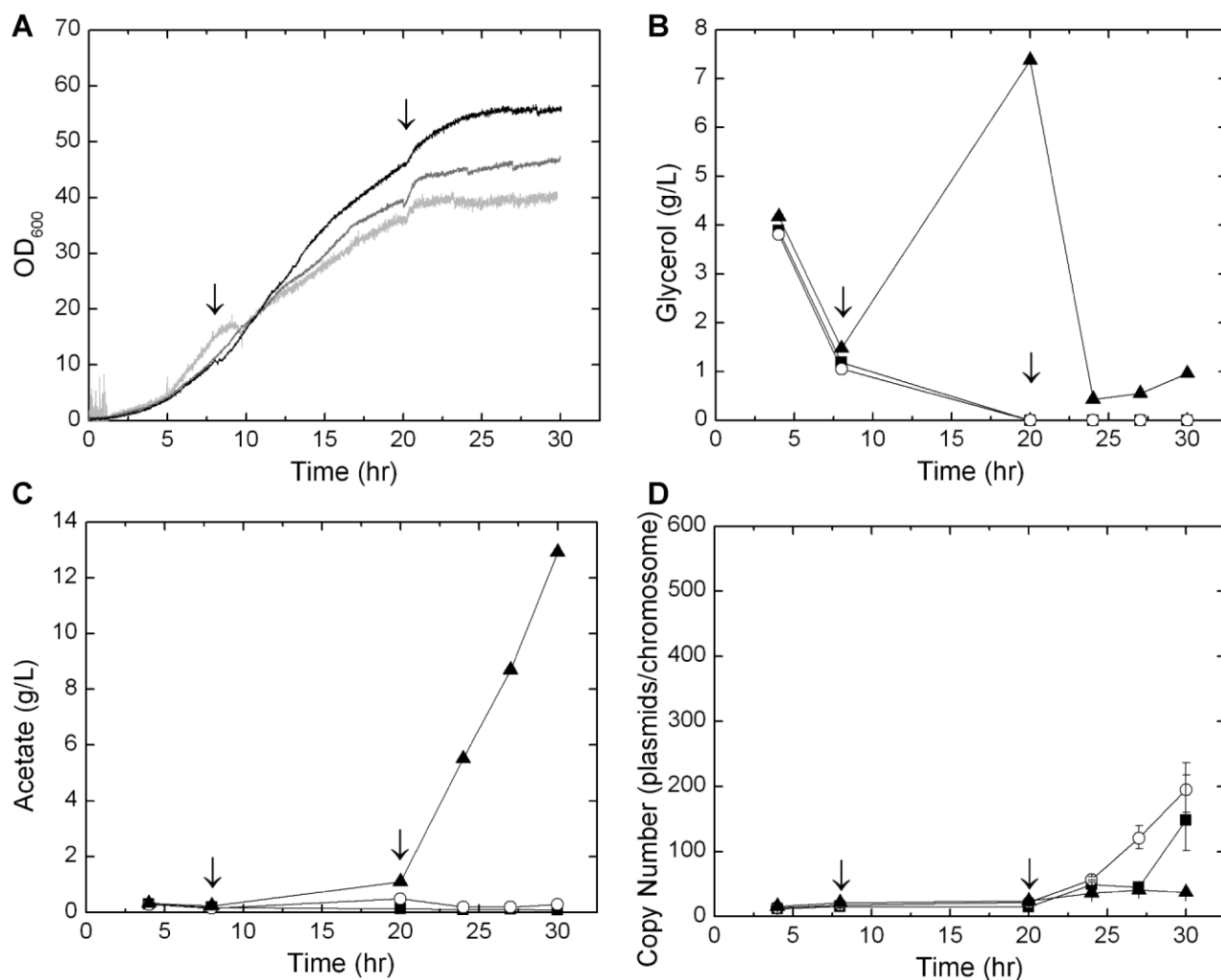


Figure 3. (A) Growth curves for the microreactor cultures at feed injection rates of 0.536 (light gray), 0.664 (dark gray), and 0.868 (black) injections per minute. (B) Glycerol, (C) acetate, and (D) average plasmid copy number profiles for microreactor fed-batch cultures with feed injection rates of 0.536 (■), 0.664 (○), and 0.868 (▲) injections per minute. In each plot, from left to right, the arrows indicate the start of feeding and the 30 to 42°C temperature shift, respectively. The plasmid copy number error bars represent the 95% confidence interval calculated from three replicate wells of the same sample.

Plasmid Quality Assessment

Plasmid DNA quality was evaluated using gel electrophoresis to demonstrate that the microreactor could produce both comparable quantity and quality (i.e., degree of supercoiling) of the product. The plasmid produced at both scales was predominantly in the supercoiled form with traces of the nicked (open-circular) form (Fig. 4). We can conclude that the microreactor cultivation does not negatively impact plasmid quality, and that the device can be used to evaluate product quality, in addition to product yield, under a variety of culture conditions.

Impact of Oxygen Availability

One of the most marked differences between the microreactor and bench-scale bioreactor studies was acetate

production. In the microreactors, acetate production was only observed when glycerol accumulated in the medium, which points to metabolic overflow as the primary cause. In contrast, acetate was produced in all of the bioreactor runs despite an absence of glycerol accumulation at all but the highest feed rate. Two common causes of acetate production are metabolic overflow (i.e., carbon flux that exceeds the capacity of the TCA cycle) and oxygen limitation (Wolfe, 2005). Elevated temperature has also been shown to induce increased acetate production (Luders et al., 2009). The degree of metabolic overflow is related to feed rate rather than scale, and the cultures were exposed to the same temperature extremes at both scales. Therefore, the most plausible explanation for the differences in acetate production likely involves the oxygen transport properties of each system. The oxygen mass transfer rate (k_La) in microreactors with the same growth chamber geometry as those

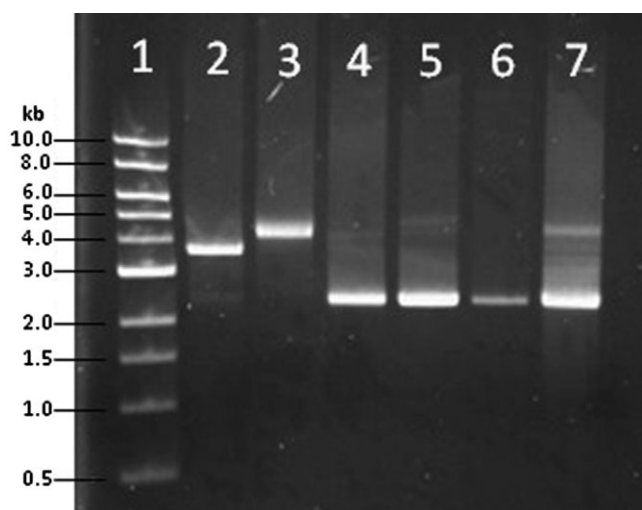


Figure 4. Agarose gel electrophoresis of plasmid DNA produced by the microreactors and bench-scale bioreactors. **Lane 1:** DNA ladder with DNA size in kilobases (kb) indicated to the left of the image, **Lane 2:** Linearized pVAX1-GFP, **Lane 3:** Nicked pVAX1-GFP, **Lane 4:** pVAX1-GFP from bench-scale reactor (3.5 g glycerol/L/h), **Lane 5:** pVAX1-GFP from bench-scale reactor (2.6 g glycerol/L/h), **Lane 6:** pVAX1-GFP from microreactor (0.868 injections/min), and **Lane 7:** pVAX1-GFP from microreactor (0.536 injections/min). Only a representative set of pDNA samples is shown. pDNA from all feed rates had quality similar to or better than that shown. All samples were from the final timepoint of each culture (approximately 30 h after inoculation). Note also that the pDNA in Lanes 4, 5, and 7 was purified from $OD_{600} = 2$ pellets, whereas the number of cells used for the pDNA preparation in Lane 6 was not determined.

used in this work has been measured previously to be approximately 58 h^{-1} (Lee et al., 2011), which is an order of magnitude lower than values typically achieved in stirred-tank vessels (Bareither and Pollard, 2011; Islam et al., 2008). To compensate for the lower k_{La} , the microreactors were always supplemented with up to 100% oxygen, resulting in different dissolved oxygen profiles at each scale (Fig. 5).

In the microreactors, the cultures were never oxygen limited for an extended period of time. Because of the intermittent nature of the feed injections, the dissolved oxygen dropped sharply immediately after the injection of substrate, but recovered before the next injection, resulting in an average dissolved oxygen concentration that was greater than zero (Fig. 5A). The same was not true for the bioreactor cultures. At the bench-scale, the setpoint was maintained until the agitation reached its maximum, at which point the oxygen demand outstripped supply and the dissolved oxygen dropped to zero (Fig. 5B). The differences in dissolved oxygen profiles across scales suggest that acetate accumulation at the bench scale could be due to the culture no longer being fully aerobic. Alexeeva et al. (2002) have shown that the acetate production rate of a culture increases dramatically during the transition from aerobic to anaerobic growth. Our hypothesis is also supported by the detection of fermentation products (formate, lactate,

succinate, and ethanol) in the medium at the highest feed rate (i.e., conditions in which the duration of zero dissolved oxygen was the longest).

Bench-scale Bioreactors With Oxygen Supplementation

To test the impact of oxygen availability on acetate accumulation and plasmid yield, we supplemented the inlet air to the bench-scale bioreactor with oxygen in order to maintain the dissolved oxygen setpoint for the entire run (Fig. 5B). Two conditions were tested: a moderate feed rate, which did not result in glycerol accumulation (3.2 g glycerol/L/h initial specific feed rate) and a high feed rate that resulted in significant glycerol accumulation (6.1 g glycerol/L/h initial specific feed rate). The glycerol profile at the moderate feed rate with oxygen supplementation (Fig. 6B) was the same as the profile with air only (Fig. 2B). At the high feed rate, the glycerol profile (Fig. 6B) resembles that observed in the microreactors at the highest feed rate tested (Fig. 3B)—glycerol accumulated after the start of the feed, but the concentration decreased after the 30 to 42°C temperature shift.

Interestingly, at the moderate feed rate with oxygen supplementation no acetate was produced after the start of feeding (Fig. 6C), in contrast to the air-only run at the same feed rate that resulted in production of approximately 7 g/L acetate (Fig. 2C). This suggests that oxygen limitation was the cause of the discrepancies in acetate production between scales. At the high feed rate with oxygen supplementation, acetate still accumulated in the medium (Fig. 6C), likely due to metabolic overflow. This is consistent with the acetate profile seen in the microreactor at the highest feed rate (Fig. 3C).

Oxygen supplementation of the bench-scale reactor led to significantly lower plasmid copy numbers (Fig. 6D) when compared to the runs with air only in the inlet gas (Fig. 2D). Some temperature-induced amplification was observed at both the moderate and high feed rates. The trends are consistent with those observed in the microreactor, in which the highest feed rate gave the lowest final copy number (Fig. 3D). The phenomenon of lower plasmid copy number under non-limiting oxygen conditions is also consistent with the low copy number observed at the lowest feed rate in the air-only bench-scale run (Fig. 2D). In this run, the dissolved oxygen setpoint could not be maintained at 30%, but remained above zero for the duration of the run.

The data from the oxygen-supplemented bioreactors clearly demonstrate that our fed-batch microreactor platform can replicate a complex bench-scale fed-batch process as long as key process parameters (i.e., oxygen availability) are held constant across scales. We have shown that the dissolved oxygen profiles under standard operating conditions can be quite different at the bench and micro-scale, and that results were only consistent across scales when these differences were accounted for. Thus, the

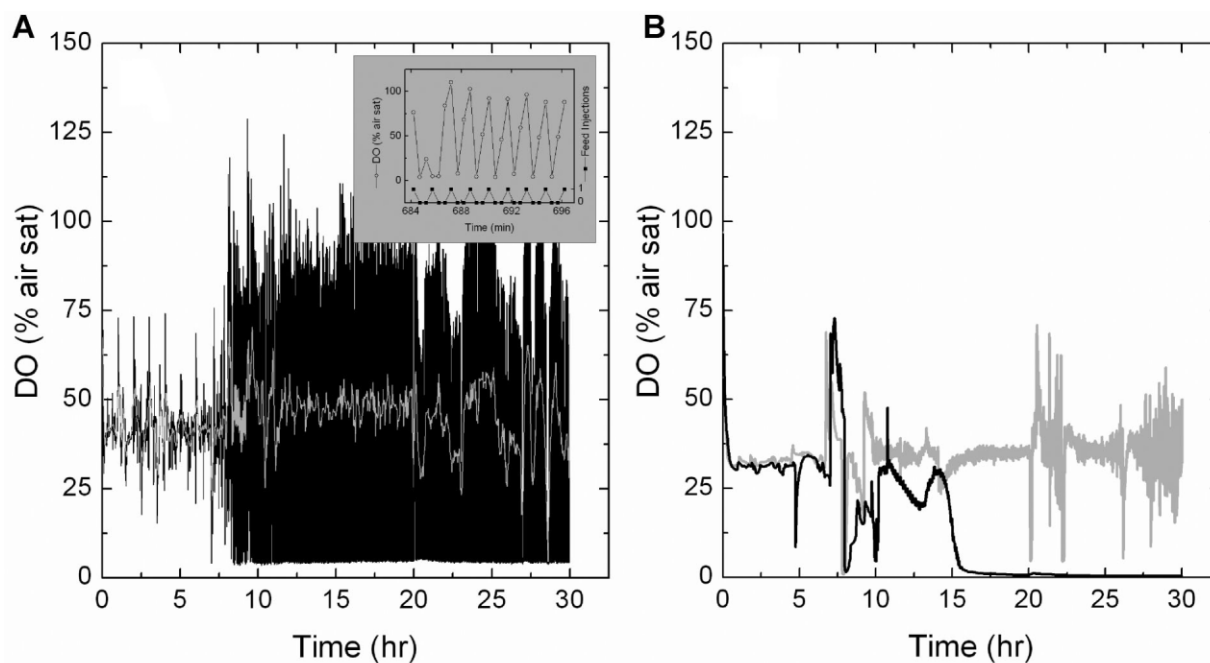


Figure 5. Dissolved oxygen profiles from representative microreactor and bench-scale bioreactor cultures. **(A)** Dissolved oxygen profile from microreactor culture with 0.664 injections/min feed rate (black line). A moving average over a 20-point window is also shown for clarity (light gray line). The inset shows a zoomed-in version of the dissolved oxygen versus time plot overlaid with the feed injection profile. For each point in the feed injection profile, a value of 0 indicates that no feed injection took place at that time, while a value of 1 indicates that a feed injection took place. **(B)** Dissolved oxygen profiles from bench-scale bioreactor cultures at an initial specific feed rate of 3.2 g glycerol/L/h with air only in the inlet gas (black line) and with oxygen supplementation (light gray line).

microreactor system enabled the identification of oxygen availability as a key parameter affecting pDNA production.

Conclusions

In this work, we demonstrated the design and implementation of a 1-mL microreactor for scale-down of a complex, fed-batch process. Our microreactor provided monitoring and control of dissolved oxygen, pH, and temperature, as well as continuous monitoring of optical density. Using the model system of temperature-induced production of a plasmid DNA vaccine vector in *E. coli* we showed that the microreactor can accurately reproduce the growth, metabolite profiles, and plasmid amplification observed at the bench-scale under comparable conditions. We varied the feed rate to demonstrate that the results were reproducible across scales under conditions in which the primary substrate (glycerol) was limiting or in excess. We also observed that plasmid copy number appeared to be higher under “non-optimal” conditions (low dissolved oxygen, acetate accumulation). These key parameters would not have been identified without the use of the scale-down system; we plan to investigate this phenomenon further as part of future work defining the optimal culture conditions for plasmid production. By extending our process

monitoring beyond growth and including metabolites and product yields as indicators of scale-down accuracy, we were able to gain a better understanding of the process as a whole.

Over the course of our investigation, we identified several differences between scales, such as volume changes with feeding (or lack thereof). However, the qualitative agreement between the bench- and micro-scale data indicates that these differences are not critical for the utility of the microreactor system. In addition, oxygen availability emerged as a key parameter to achieve consistency during scale-down. The increased ease and safety of using oxygen supplementation at the microscale led us to uncover this key process requirement. Various input gas mixtures could be explored in the microreactors to further investigate the impact of oxygen availability on culture productivity.

Overall, we have demonstrated the successful scale down of a temperature-inducible, fed-batch process for plasmid DNA production in *E. coli* from 2 L to 1 mL. Our microreactor device includes many of the key features required to meet the current needs of microbial process development in the biopharmaceutical, biomaterials, and biofuels industries. These features include advanced process monitoring and control capabilities, well-controlled feeding, sufficient oxygen transfer to achieve high cell densities, and rapid set-up and clean-up. Current and future work seeks to

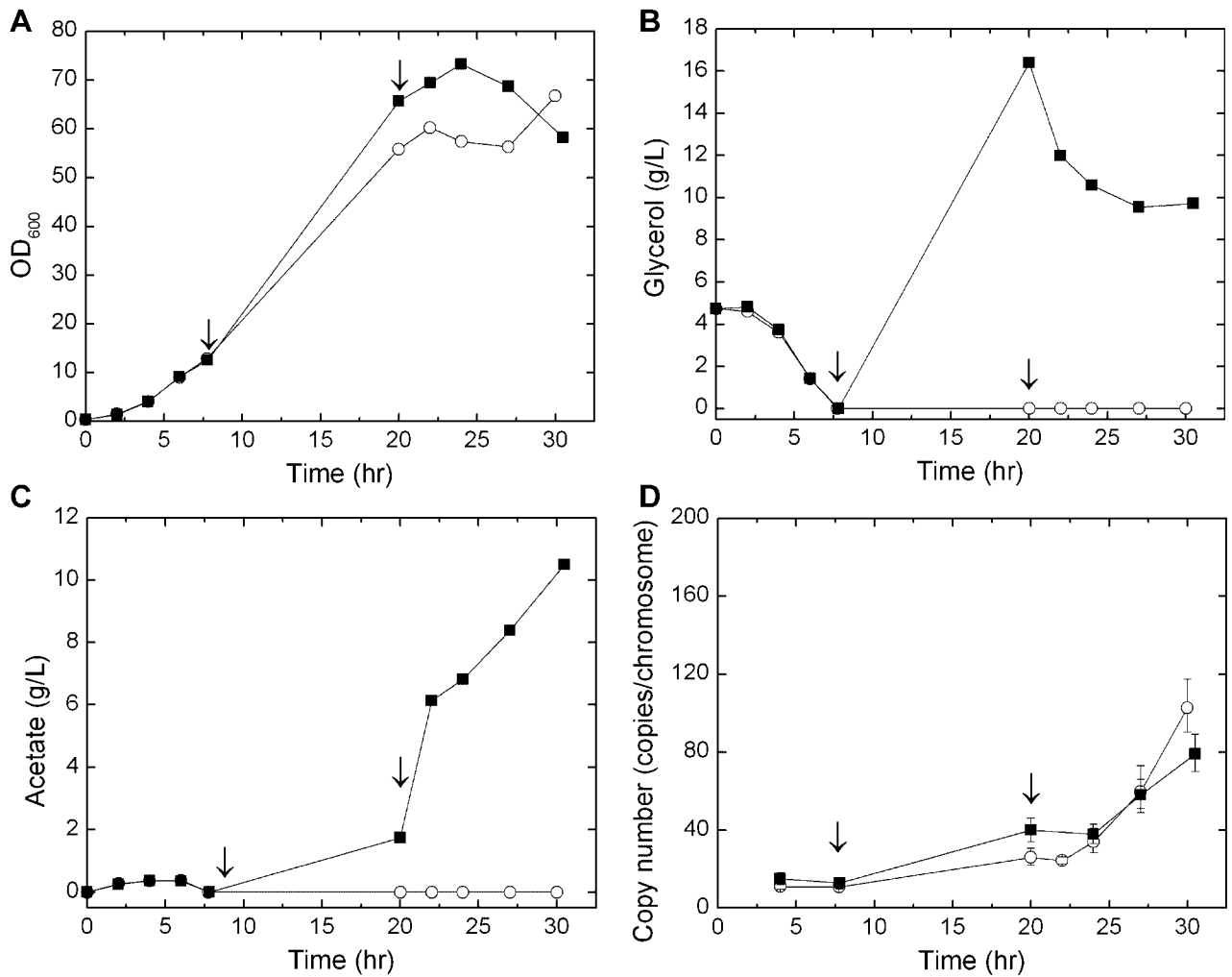


Figure 6. (A) Optical density, (B) glycerol, (C) acetate, and (D) average plasmid copy number profiles for oxygen-supplemented bench-scale cultures with initial specific feed rates of 3.2 g glycerol/L/h (○) and 6.1 g glycerol/L/h (■). In each plot, from left to right, the arrows indicate the start of feeding and the 30 to 42°C temperature shift, respectively. Error bars on the plasmid copy number values represent the 95% confidence level calculated from three replicate wells of the same sample.

parallelize the devices to allow a single researcher to run multiple experiments simultaneously.

This work was supported by funds from the MIT-Portugal Program (graduate research assistance to DMB), Pfizer, Inc. (graduate research assistance to DMB), and the National Science Foundation (KSL).

References

- Akerlund T, Nordström K, Bernander R. 1995. Analysis of cell size and DNA content in exponentially growing and stationary-phase batch cultures of *Escherichia coli*. *J Bacteriol* 177:6791–6797.
- Alexeeva S, Hellingwerf KJ, Teixeira de Mattos MJ. 2002. Quantitative assessment of oxygen availability: Perceived aerobiosis and its effect on flux distribution in the respiratory chain of *Escherichia coli*. *J Bacteriol* 184:1402–1406.
- Bareither R, Pollard D. 2011. A review of advanced small-scale parallel bioreactor technology for accelerated process development: Current state and future need. *Biotechnol Prog* 27:2–14.
- Betts JI, Baganz F. 2006. Miniature bioreactors: Current practices and future opportunities. *Microb Cell Fact* 5:21.
- Bipatnath M, Dennis PP, Bremer H. 1998. Initiation and velocity of chromosome replication in *Escherichia coli* B/r and K-12. *J Bacteriol* 180:265–273.
- Carnes AE, Hodgson CP, Williams JA. 2006. Inducible *Escherichia coli* fermentation for increased plasmid DNA production. *Biotechnol Appl Biochem* 45:155–166.
- Funke M, Buchenauer A, Mokwa W, Kluge S, Hein L, Mueller C, Kensy F, Buechs J. 2010. Bioprocess control in microscale: Scalable fermentations in disposable and user-friendly microfluidic systems. *Microb Cell Fact* 9:86.
- Isett K, George H, Herber W, Amanullah A. 2007. Twenty-four-well plate miniature bioreactor high-throughput system: Assessment for microbial cultivations. *Biotechnol Bioeng* 98:1017–1028.
- Islam RS, Tisi D, Levy MS, Lye GJ. 2008. Scale-up of *Escherichia coli* growth and recombinant protein expression conditions from microwell to laboratory and pilot scale based on matched $k_{t,a}$. *Biotechnol Bioeng* 99:1128–1139.
- Kostov Y, Harms P, Randers-Eichhorn L, Rao G. 2001. Low-cost micro-bioreactor for high-throughput bioprocessing. *Biotechnol Bioeng* 72:346–352.
- Kutzler MA, Weiner DB. 2008. DNA vaccines: Ready for prime time? *Nat Rev Genet* 9:776–788.

- Lee HLT, Boccazzi P, Gorret N, Ram RJ, Sinskey AJ. 2004. In situ bioprocess monitoring of *Escherichia coli* bioreactions using Raman spectroscopy. *Vib Spectrosc* 35:131–137.
- Lee C, Kim J, Shin SG, Hwang S. 2006a. Absolute and relative QPCR quantification of plasmid copy number in *Escherichia coli*. *J Biotechnol* 123:273–280.
- Lee HL, Boccazzi P, Ram RJ, Sinskey AJ. 2006b. Microbioreactor arrays with integrated mixers and fluid injectors for high-throughput experimentation with pH and dissolved oxygen control. *Lab Chip* 6:1229–1235.
- Lee KS, Boccazzi P, Sinskey AJ, Ram RJ. 2011. Microfluidic chemostat and turbidostat with flow rate, oxygen, and temperature control for dynamic continuous culture. *Lab Chip* 11:1730–1739.
- Legmann R, Schreyer HB, Combs RG, McCormick EL, Russo AP, Rodgers ST. 2009. A predictive high-throughput scale-down model of monoclonal antibody production in CHO cells. *Biotechnol Bioeng* 104:1107–1120.
- Listner K, Bentley LK, Chartrain M. 2006. A simple method for the production of plasmid DNA in bioreactors. In: Saltzman WM, Shen H, Brandsma JL, editors. *DNA vaccines: Methods and protocols*. Totowa, NJ: Humana Press. p 295–309.
- Livak K, Schmittgen T. 2001. Analysis of relative gene expression data using real-time quantitative PCR and the $2^{-\Delta\Delta CT}$ method. *Methods* 25:402–408.
- Luders S, Fallet C, Franco-Lara E. 2009. Proteome analysis of the *Escherichia coli* heat shock response under steady-state conditions. *Proteome Sci* 7:36.
- Neidhardt FC, Umberger HE. 1996. Chemical composition of *Escherichia coli*. In: Neidhardt FC, editor. *Escherichia coli and Salmonella: Cellular and molecular biology*, 2nd edn. Washington, DC: ASM Press. p 13–16.
- Panula-Perala J, Siurkus J, Vasala A, Wilmanowski R, Casteleijn MG, Neubauer P. 2008. Enzyme controlled glucose auto-delivery for high cell density cultivations in microplates and shake flasks. *Microb Cell Fact* 7:31.
- Pedelacq JD, Cabantous S, Tran T, Terwilliger TC, Waldo GS. 2006. Engineering and characterization of a superfolder green fluorescent protein. *Nat Biotechnol* 24:79–88.
- Schäpper D, Alam MNHZ, Szita N, Lantz AE, Gernaey KV. 2009. Application of microbioreactors in fermentation process development: A review. *Anal Bioanal Chem* 395:679–695.
- Siurkus J, Panula-Perala J, Horn U, Kraft M, Rimseliene R, Neubauer P. 2010. Novel approach of high cell density recombinant bioprocess development: Optimisation and scale-up from microlitre to pilot scales while maintaining the fed-batch cultivation mode of *E. coli* cultures. *Microb Cell Fact* 9:35.
- Vester A, Hans M, Hohmann H, Weuster-Botz D. 2009. Discrimination of riboflavin producing *Bacillus subtilis* strains based on their fed-batch process performances on a millilitre scale. *Appl Microbiol Biotechnol* 84:71–76.
- Wolfe AJ. 2005. The acetate switch. *Microbiol Mol Biol Rev* 69:12–50.